International Journal of Automation and Computing 10(1), February 2013, 73-78
DOI: 10.1007/s11633-013-0698-9

H_∞ Robust Control of DC-AC Interfaced Microsource in Microgrids

Chun-Xia Dou Fang Zhao Xing-Bei Jia Dong-Le Liu
Institute of Electrical Engineering, Yanshan University, Qinhuangdao 066004, China

Abstract: This paper focuses on the direct current - alternating current (DC-AC) interfaced microsource based H_∞ robust control strategies in microgrids. It presents detail of a DC-AC interfaced microsource model which is connected to the power grid through a controllable switch. A double loop current-regulated voltage control scheme for the DC-AC interface is designed. In the case of the load disturbance and the model uncertainties, the inner voltage and current loop are produced based on the H_∞ robust control strategies. The outer power loop uses the droop characteristic controller. Finally, the scheme is simulated using the Matlab/Simulink. The simulation results demonstrate that DC-AC interfaced microsource system can supply high quality power. Also, the proposed control scheme can make the system switch smoothly between the isolated mode and grid-connected mode.

Keywords: Microgrid, DC-AC interfaced microsource, H_∞ robust control, f-v droop characteristic, smooth switching.

1 Introduction

For economic, technical and environmental reasons, the microgrid, powered by microsource, such as fuel cells[1], photovoltaic cells, and microturbines, is becoming widely used[2−3]. The microgrid concept refers to a system which coordinates local level energy supply and demand. It provides a platform for the integration of various distributed energy resources through a communication system enabling control actions. The microgrid can be connected to an upper level utility power grid, but it is also capable of operating in a disconnected island mode.

The consortium for electric reliability technology solutions (CERTS) microgrid concept is driven by the following principles[4]:

1) A systems perspective is necessary for customers, utilities, and society to capture the full benefits of integrating distributed energy resources into an energy system;

2) The business case for accelerating adoption of these advanced concepts will be driven, primarily by lowing the cost and enhancing the value of microgrids.

In the actual operation of microgrids, the key issue is control of the DC-AC interfaced microsource[5, 6]. The DC-AC interface is used to connect the microsource to the utility grid. It is important[7] as:

1) It improves power quality by providing extremely fast switching times for sensitive loads;

2) It provides reactive power control and voltage regulation at the microgrids system connection point;

3) It reduces or eliminates fault current effect on microgrids system, thereby, it allows negligible impacts on protection coordination;

4) It provides flexibility in operations with various other microgrids sources, and reduces overall interconnection costs through standardization and modularity.

The operation and control of a DC-AC interfaced microsource present great challenge for the microgrids. Particularly smooth switching between the isolated mode and grid-connected mode has to be carefully designed in the case of voltage and frequency fluctuations. Also, the control of electrical generator and DC-AC interface will play an important role in the overall control system in microgrid. Different from the conventional large power system, there are not grid voltage and frequency to reference. In this case, the control and operation of DC-AC interface become a great concern in such system design.

There are many control schemes for the power electronic interfaced microsource[8−12]. Brabandere et al.[8] discussed the voltage and frequency control operations are particularly discussed. They also implemented control concepts of microgrids. Besides, Brabandere et al.[9] described a voltage and frequency droop control method for parallel operation of inverters operating in an island grid or connected to an infinite bus. A detailed analysis shows that this approach has a superior behavior compared to the existing methods. Also, a detail of H_∞ repetitive control of DC-AC converters in microgrids is given in [10]. The repetitive control is used to reject harmonic disturbances from nonlinear loads or the public grid, and H_∞ method is to ensure that the controller performs effectively with a range of local load impedances. Serban et al.[11] proposed a control strategy for a distributed power generation microgrid application. Feng and Chen[12] presented the control strategy of power electronics interfaced distribution generation units.

This paper proposes an H_∞ robust[13−15] control scheme for DC-AC interfaced microsource. For the purpose of designing this control scheme, the system powers are firstly obtained via required voltage and frequency. Based on three-phase grid-connected power system model, which is developed for the overall power system including the DC-AC interface, the control scheme is designed as a double loop current-regulated voltage control. In this research, one of the critical challenges was to make the system switch smoothly between the isolated mode and grid-connected

Manuscript received January 13, 2011; revised March 14, 2012
This work was supported by National Natural Science Foundation of China (No. 51177142), China Postdoctoral Science Foundation (Nos. 2012T50019 and 20110490210), Hebei Provincial Natural Science Foundation of China (No. F2012203063).

mode. The overall system, consisting of a microsource with DC-AC interface, is simulated in the Matlab/Simulink. The performance of the double loop control scheme was thoroughly tested and analyzed by the simulation study, and is systematically presented in the paper.

2 System modeling

2.1 A three-phase grid-connected DC-AC interfaced system

Fig. 1 shows the system to be controlled. This system consists of microsource, DC-AC inverter (IGBT bridge), LCL filters, the local consumers, controllable switch and the power grid. The DC-AC inverter is used to transform the direct current into alternating current. The LCL filter connected at the inverter terminals are to filter out the harmonics at the switching frequency 4 kHz. The controllable switch can make the microgrid connect or disconnect to the power grid. The microgrid connects to the power grid through the transformer.

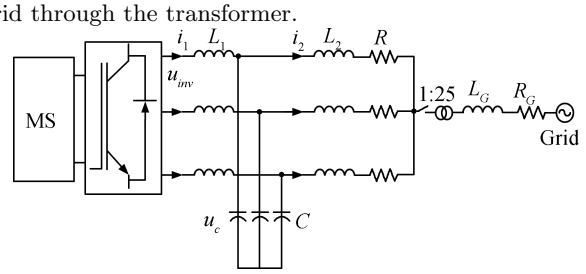

Fig. 1 Three-phase grid-connected power system diagram

2.2 The state-space model of the power system

The state-space model of the island microgrid is

$$\begin{aligned}\frac{\mathrm{d}i_1}{\mathrm{d}t} &= -\frac{1}{L_1}u_c + \frac{1}{L_1}u_{inv}\\ \frac{\mathrm{d}i_2}{\mathrm{d}t} &= -\frac{R}{L_2}i_2 + \frac{1}{L_2}u_c\\ \frac{\mathrm{d}u_c}{\mathrm{d}t} &= -\frac{1}{C}i_2 + \frac{1}{C}i_1\end{aligned} \tag{1}$$

where u_{inv} is output voltage of the inverter, i_1 is output current of the inverter, u_c is voltage of the filter capacitor, i_2 is current of the load, L_1, L_2, C are capacitance and inductance of the filter.

The output equation is

$$z = Ri_2 - u_{\mathrm{ref}} \tag{2}$$

where u_{ref} is reference voltage. Equations (1) and (2) represent the system model and output in state space variables, which can be shown in the following matrix form

$$\begin{cases}\dot{x}(t) = Ax(t) + Bu(t)\\ z(t) = Cx(t)\end{cases} \tag{3}$$

where

$$A = \begin{bmatrix} 0 & 0 & -\dfrac{1}{L_1}\\ 0 & -\dfrac{R}{L_2} & \dfrac{1}{L_2}\\ \dfrac{1}{C} & -\dfrac{1}{C} & 0\end{bmatrix},$$

$$B = \begin{bmatrix}\dfrac{1}{L_1}\\ 0\\ 0\end{bmatrix},\ C = \begin{bmatrix} 0 & R & 0\end{bmatrix},$$

$$x^{\mathrm{T}}(t) = \begin{bmatrix} i_1 & i_2 & u_c\end{bmatrix},$$

$$u(t) = [u_{inv}].$$

In an actual power system, the nonlinear load, phase asymmetry and other factors must be taken into account. Here, we introduce the parametric uncertainty. We consider the major parameter R as ΔR, (3) can be generalized as

$$\begin{cases}\dot{x}(t) = (A + \Delta A(t))x(t) + Bu(t)\\ z(t) = Cx(t) + D\omega(t).\end{cases} \tag{4}$$

The uncertainty matrix is

$$\Delta A(t) = \begin{bmatrix} 0 & 0 & 0\\ 0 & -\eta(t) & 0\\ 0 & 0 & 0\end{bmatrix}$$

where $\eta(t) = \Delta R L_2$. For the purpose of illustration, the parametric perturbation is considered as $\Delta R = 0.15R$.

3 Controller design

From the state-space model mentioned above, it is obvious that the essential task is to control the output voltage at required magnitude and frequency.

Fig. 2 shows the complete control system of the microsource. The inputs of the control system are either measurements (e.g., the voltages and currents) or set points (e.g., voltage, power and the nominal grid frequency). The outputs are the gate pulses that describe when and for how long the power electronic devices are going to conduct. The inverter voltage and current along with the load voltage are measured. The voltage magnitude at the load bus and the active power injected are then calculated.

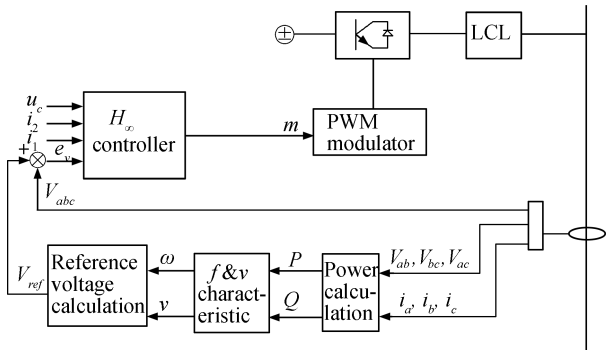

Fig. 2 Final version of microsource control

As shown in Fig. 2, V_{abc} is the root mean square (RMS) line-to-neutral voltage, i_{abc} is the RMS line current, V_{ab}, V_{bc}, V_{ac} are line-to-line voltage, i_a, i_b, i_c are line current, P and Q are the calculated active power and reactive power. The controller of the inverter is a double-loop controller. In this control strategy, the inner loop is a voltage and current regulation loop, and the outer loop is a power regulation loop. First, V_{ab}, V_{bc}, V_{ac} and i_a, i_b, i_c are measured, and through the power calculation module we can obtain the active power P and reactive power Q. Then, we analyze the f-v characteristic, and gain the voltage phase angle ω and magnitude v. Finally, the reference voltage u_{ref} is calculated. Here, we use the H_∞ controller to regulate the inner voltage and current loops, and use the droop characteristic controller for the outer loop. This paper mainly describes the design of the H_∞ controller, which is designed in the subsequent section.

3.1 Power calculation

The power calculation module is used to calculate the values of active and reactive power. In order to complete the calculation, we will use the instantaneous values of line to line voltages and line currents. These quantities can be brought in from the measuring equipment. The voltages are always measured across the phases in case that there is no ground to refer to. We should measure only two of the line to line voltages and calculate the third one from the fact that the sum of the three delta voltages must equal zero, in balanced as well as under unbalanced conditions. With respect to the currents, we should only measure two currents and the third one is calculated assuming their overall sum is zero, but which is correct only under balanced conditions.

The calculation of P and Q are

$$\begin{aligned} P &= V_{bc}i_c - V_{ab}i_a \\ Q &= -\frac{V_{bc}(2i_a + i_b) + V_{ca}(2i_b + i_a)}{\sqrt{3}}. \end{aligned} \tag{5}$$

One advantage of adopting (5) is that the variables are readily available, such as voltages denote the line to line voltage so that there is no need to convert them to line to neutral. Another advantage is the simplicity of the equations that do not require the extra step of being converted to rotating frame components, since the powers are evaluated from the immediately available time domain quantities obtained from the sensing equipment.

3.2 *f* & *v* characteristic

This section will give the detail of f-v droop characteristic and the selection of the voltage-frequency drop coefficients m and n. Chandorker et al.[16] proposed a method to regulate the power-frequency (P, ω) characteristic and reactive power-voltage (Q-v) characteristic. This method can make each microsource supply active and reactive power in proportion with its power rating. The equations are

$$\begin{aligned} \omega &= \omega_0 - m \cdot P \\ v &= v_0 - n \cdot Q \end{aligned} \tag{6}$$

where the droop coefficients m and n can expressed as

$$\begin{aligned} m &= \frac{\omega_0 - \omega_{\min}}{p_0 - p_{\max}} \\ n &= \frac{v_0 - v_{\min}}{Q_0 - Q_{\max}} \end{aligned} \tag{7}$$

where ω_0 is the operation frequency when there is no load in the system ($p_0 = 0$), $p_{\max}$, $\omega_{\min}$ are the maximum active power output of microsource system and the minimum operation frequency. v_0 is the initial value of voltage magnitude, it is set as 318.2 V (225 V phase voltage). Q_0 is the initial reactive power, it is set as zero. $Q_{\max}, v_{\min}$ are the maximum reactive power output of microsource system and the minimum voltage magnitude.

Then, the three-phase reference voltage can be expressed as

$$\begin{aligned} V_{\text{ref},a} &= v \cdot \cos(\omega \cdot t) \\ V_{\text{ref},b} &= v \cdot \cos(\omega \cdot t - 120^\circ) \\ V_{\text{ref},c} &= v \cdot \cos(\omega \cdot t + 120^\circ). \end{aligned} \tag{8}$$

3.3 H_∞ robust controller design

This section will design the H_∞ robust controller. The state-space model of the system is (4), which is showed in Section 2.

Assumption 1. The parameter uncertainty ΔA satisfies the matching condition:

$$\Delta A = E\Sigma(t)F$$

where E and F are the constant real matrices with appropriate dimensions, and $\Sigma(t)$ is an unknown function matrix and satisfies $\Sigma^{\mathrm{T}}(t)\Sigma(t) \leqslant I$, in which I is a unit matrix.

According to Assumption 1, the parameter uncertainties can be expressed as

$$\begin{aligned} E &= [0 \quad 0 \quad 1]^{\mathrm{T}} \\ \Sigma(t) &= \begin{bmatrix} 0 & \dfrac{\eta(t)}{|\eta(t)|} & 0 \end{bmatrix} \\ F &= \begin{bmatrix} 0 & 0 & 0 \\ 0 & -|\eta(t)| & 0 \\ 0 & 0 & 0 \end{bmatrix}. \end{aligned}$$

For system (6), we consider the state feedback

$$u = Kx(t). \tag{9}$$

The closed-loop system is obtained as

$$\begin{cases} \dot{x}(t) = [A + BK + E\Sigma(t)F]x(t) \\ z(t) = Cx(t) + D\omega(t). \end{cases} \tag{10}$$

Define Lyapunov function of this system as

$$V(t) = x^{\mathrm{T}}(t)Px(t)$$

where P is a symmetric positive definite weighting matrix.

Without considering the initial condition, the performance of H_∞ is related to the transfer function $T_{z\omega}(s)$ in the following form

$$\|T_{z\omega}(s)\|_\infty < \gamma \tag{11}$$

where γ is a constant representing prescribed attenuation level. $T_{z\omega}(s)$ is the transfer function from $\omega(t)$ to $z(t)$.

Theorem 1. The control system of (4) has a state feedback controller to make the closed-loop system (10) asymptotically stable and possess the control performance in (11), if and only if $P = P^{\mathrm{T}} > 0$ satisfies the following matrix inequality

$$\begin{bmatrix} \hat{A}^{\mathrm{T}}P + P\hat{A} & 0 & C^{\mathrm{T}} \\ 0 & -\gamma & D^{\mathrm{T}} \\ C & D & -\gamma \end{bmatrix} < 0 \tag{12}$$

where P is a symmetric positive definite weighting matrix, $\hat{A} = A + BK + E\Sigma(t)F$.

Proof. Let us left multiply and right multiply diagonal matrix diag $\{\gamma^{1/2}I, \gamma^{1/2}I, \gamma^{-1/2}I\}$ into the matrix inequality (12), and denote $X = \gamma P > 0$, then the equivalent inequality is changed as follows

$$\begin{bmatrix} \hat{A}^{\mathrm{T}}X + X\hat{A} & 0 & C^{\mathrm{T}} \\ 0 & -\gamma^2 & D^{\mathrm{T}} \\ C & D & -I \end{bmatrix} < 0. \tag{13}$$

Then, we obtain $\hat{A}^{\mathrm{T}}X + X\hat{A} < 0$, so system (4) is asymptotically stable, and $V(t) = x^{\mathrm{T}}(t)Xx(t)$ is a Lyapunov function for the system (4). We select an appropriate constant $0 < \lambda < 1$ satisfying the following matrix inequality

$$\begin{bmatrix} \hat{A}^{\mathrm{T}}X + X\hat{A} & 0 & C^{\mathrm{T}} \\ 0 & -\gamma^2(1-\lambda) & D^{\mathrm{T}} \\ C & D & -I \end{bmatrix} < 0. \tag{14}$$

By the Schur complement theorem, the above inequality (14) is equivalent to (15)

$$\begin{bmatrix} C^{\mathrm{T}} \\ D^{\mathrm{T}} \end{bmatrix} [C \;\; D] + \begin{bmatrix} \hat{A}^{\mathrm{T}}X + X\hat{A} & 0 \\ 0 & -\gamma^2(1-\lambda) \end{bmatrix} < 0. \tag{15}$$

For any $T > 0$, consider

$$J_T = \int_0^T \|z\|^2 \mathrm{d}t - (1-\lambda)\gamma^2 \int_0^T \|\omega\|^2 \mathrm{d}t.$$

Under the zero initial state conditions,

$$J_T = \int_0^T [z^{\mathrm{T}}(t)z(t) - (1-\lambda)\gamma^2\omega^{\mathrm{T}}(t)\omega(t)]\mathrm{d}t =$$
$$\int_0^T [z^{\mathrm{T}}(t)z(t) - (1-\lambda)\gamma^2\omega^{\mathrm{T}}(t)\omega(t) + \dot{V}(x(t))]\mathrm{d}t -$$
$$V(x(T)) =$$
$$\int_0^T [z^{\mathrm{T}}(t)z(t) - (1-\lambda)\gamma^2\omega^{\mathrm{T}}(t)\omega(t) +$$
$$2x^{\mathrm{T}}(t)X\hat{A}x(t)]\mathrm{d}t - V(x(T)) =$$
$$\int_0^T \begin{bmatrix} x(t) \\ \omega(t) \end{bmatrix}^{\mathrm{T}} \left(\begin{bmatrix} C^{\mathrm{T}} \\ D^{\mathrm{T}} \end{bmatrix} \begin{bmatrix} C & D \end{bmatrix} + \begin{bmatrix} \hat{A}^{\mathrm{T}}X + X\hat{A} & 0 \\ 0 & -\gamma^2(1-\lambda) \end{bmatrix} \right) \begin{bmatrix} x(t) \\ \omega(t) \end{bmatrix} \mathrm{d}t - V(x(T)).$$

From above calculation result and (15), we can obtain

$$\int_0^T [z^{\mathrm{T}}(t)z(t) - (1-\lambda)\gamma^2\omega^{\mathrm{T}}(t)\omega(t) + \dot{V}(x(t))]\mathrm{d}t < 0.$$

Take the advantage of the zero initial state conditions again, the calculation result of the above inequality is as

$$x^{\mathrm{T}}(T)Xx(T) + \int_0^{\mathrm{T}} \|z(t)\|^2 \mathrm{d}t < (1-\lambda)\gamma^2 \int_0^{\mathrm{T}} \|\omega(t)\|^2 \mathrm{d}t.$$

By the asymptotic stability of the system and $\omega \in L_2[0, \infty)$, let $T \to \infty$ in above inequality, we can obtain

$$\|z(t)\|_2^2 < (1-\lambda)\gamma^2\|\omega(t)\|_2^2 < \gamma^2\|\omega(t)\|_2^2.$$

The above inequality is equivalent to (11). □

In (12), $\Sigma(t)$ is an unknown matrix function, we should deal with the parameter uncertainty problem as follows.

Lemma 1. For matrices (or vectors) Y, D and E with appropriate dimensions, we have

$$Y + DFE + E^{\mathrm{T}}F^{\mathrm{T}}D^{\mathrm{T}} < 0$$

where Y is a symmetric matrix. For all F satisfying $F^{\mathrm{T}}F < I$, if and only if a set of scalar quantity $\varepsilon > 0$ exists, we gain

$$Y + \varepsilon DD^{\mathrm{T}} + \varepsilon^{-1}E^{\mathrm{T}}E < 0.$$

Theorem 2. The system (10) is asymptotically stable by the control action as (9) and it possesses the H_∞ controller performance in (11) for a prescribed γ, if and only if a set of scalar quantity $\beta > 0$ and $P = P^{\mathrm{T}} > 0$ satisfies the following matrix inequality.

$$\begin{bmatrix} \Phi + \beta PEE^{\mathrm{T}}P & 0 & C^{\mathrm{T}} & F^{\mathrm{T}} \\ 0 & -\gamma & D^{\mathrm{T}} & 0 \\ C & D & -\gamma & 0 \\ F & 0 & 0 & -\beta I \end{bmatrix} < 0 \tag{16}$$

where $\Phi = P(A + BK) + (A + BK^{\mathrm{T}}P$.

Proof. Denote

$$Y = \begin{bmatrix} \Phi & 0 & C^{\mathrm{T}} \\ 0 & -\gamma & D^{\mathrm{T}} \\ C & D & -\gamma \end{bmatrix}. \tag{17}$$

By the equation

$$\hat{A}^{\mathrm{T}}P + P\hat{A} = \Phi + PE\Sigma(t)F + F^{\mathrm{T}}\Sigma^{\mathrm{T}}(t)E^{\mathrm{T}}P$$

the matrix inequality (12) is equivalent to

$$Y + \begin{bmatrix} PE \\ 0 \\ 0 \end{bmatrix} \Sigma(t)[F \;\; 0 \;\; 0] + [F \;\; 0 \;\; 0]^{\mathrm{T}}\Sigma^{\mathrm{T}}(t) \begin{bmatrix} PE \\ 0 \\ 0 \end{bmatrix}^{\mathrm{T}} < 0.$$

According to Lemma 1, for all $\Sigma(t)$ satisfying $\Sigma^{\mathrm{T}}(t)\Sigma(t) \leqslant I$, if and only if a set of scalar quantity $\beta > 0$ exist, the following inequality is satisfied

$$Y + \beta \begin{bmatrix} PE \\ 0 \\ 0 \end{bmatrix} [0 \;\; 0 \;\; E^{\mathrm{T}}P] + \beta^{-1} \begin{bmatrix} F^{\mathrm{T}} \\ 0 \\ 0 \end{bmatrix} [F \;\; 0 \;\; 0] < 0.$$

By the Schur complement, the above inequality is equivalent to (16). □

Remark 1. In order to obtain better robust performance, the H_∞ control performance can be treated as the following minimization problem so that the performance of H_∞ in (11) is reduced as small as possible.

$$\begin{aligned} &\min \gamma \\ &\text{s.t.} \quad \begin{array}{l} 1)\ \text{Inequality (16)}; \\ 2)\ P = P^{\mathrm{T}} > 0. \end{array} \end{aligned} \tag{18}$$

The above minimization problem (18) can be transformed into LMI problem. Then, we can use the convex optimization techniques of LMI in Matlab toolboxes to design the controller.

4 Simulation results

The simulation studies have been performed. The simulation parameters are listed in Table 1.

Table 1 Simulation parameters of the overall system

Components	Parameters	Symbols	Quantity
DG system	Nominal frequency	f	50 Hz
	Nominal RMS phase voltage	V	200 V
Converter LC filter	Inductance	L_1	2 mH
	Capacitance	C	100 μF
AC Bus	Resistance	R	0.01 Ω
	Inductance	L_2	2 mH
Grid	Voltage		10 kV
	Resistance	R_G	0.34 Ω
	Inductance	L_G	2 mH
Controller	Frequency-droop characteristics	m	0.0000094
	Voltage-droop characteristics	n	0.000177

In order to investigate the performance of the proposed controller in response to OR against sudden changes within an islanded network, simulation examples are given in this section. Initially, microgrid was connected to the power grid and worked in the grid-connect mode. At $t = 3$, the microgrid broke away from the power grid and worked in the isolated mode.

The simulation results are shown in Fig. 3. Figs. 3 (a) and (b) reflect the power changes during the period when the microgrid is broken away from the distribution network. Initially, the microgrid absorbed partial active power from the grid, so when it was broken away from the grid, the active power output by the microsource was increased. According to Fig. 3 (c), we know the load voltage is still in stable condition. In Fig. 3 (d), the frequency decreased in the case of the active power increase. According to the results, we draw the conclusion that the control scheme can make the system switch smoothly from the isolated mode to grid-connected mode.

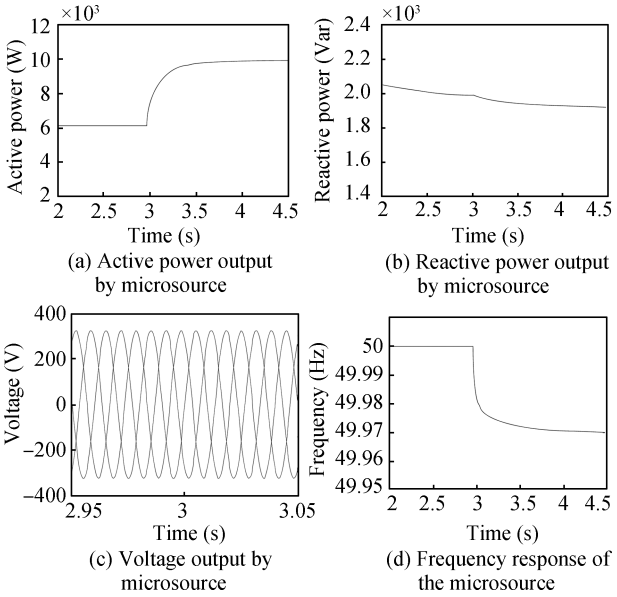

Fig. 3 Response curves when microsouce is disconnected

At $t = 4.5$, the microgrid reconnected to the power grid and worked in the grid-connected mode again. The simulation results are shown in Fig. 4.

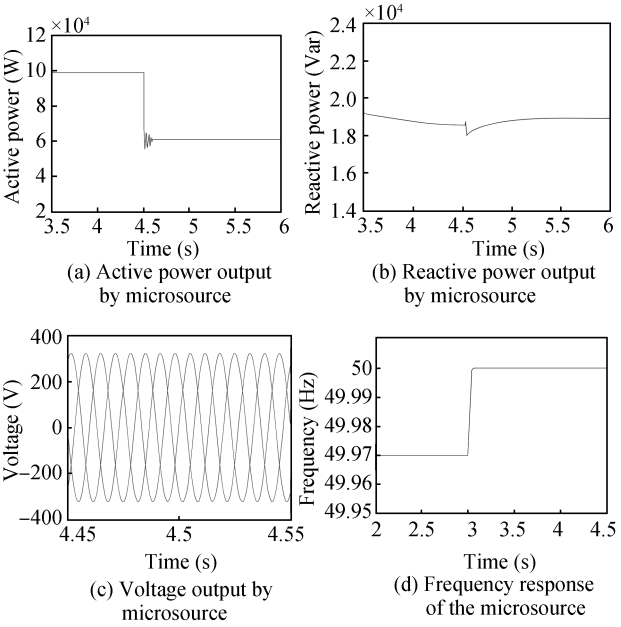

Fig. 4 Response curves when microsouce is reconnected

Figs. 4 (a) and (b) reflect the active power was decreased and the reactive power was increased during the period when the microgrid was reconnected with the distribution network. According to Fig. 4 (c), we know the load voltage is still in stable condition. In Fig. 4 (d), the frequency increased in the case of the active power decreased. According to the results, we draw the conclusion that the control scheme can make the system switch smoothly from the grid-connected mode to isolated mode.

5 Conclusions

This paper has presented a detailed study of a microgrid system connected with DC-AC interface. A double loop control system for the interface is developed. The H_∞ control scheme is designed including the inner voltage/current loop and the outer droop characteristic based power loop. The control performance of the proposed DC-AC interfaced microsource was tested through simulation examples in the Matlab/Simulink software environment. The results show that it is possible to use DC-AC interfaced microsource system to supply high-quality power.

Acknowledgments

The authors express their sincere gratitude to the reviewers for their constructive suggestions which help improve the presentation of this paper.

References

[1] J. G. Williams, G. P. Liu, S. C. Chai, D. Rees. Intelligent control for improvements in PEM fuel cell flow performance. *International Journal of Automation and Computing*, vol. 5, no. 2, pp. 145–151, 2008.

[2] R. H. Lasseter, P. Piagi. Microgrid: A conceptual solution. In *Proceedings of the 35th Annual Power Electronics Specialists Conference*, IEEE, Aachen, Germany, pp. 4285–4290, 2004.

[3] D. Georgakisl, S. Papathanassiou, N. Hatziargyriou, A. Engler, C. Hardt. Operation of a prototype microgrid system based on micro-sources quipped with fast-acting power electronics interfaces. In *Proceedings of the 35th Annual Power Electronics Specialists Conference*, IEEE, Aachen, Germany, pp. 2521–2526, 2004.

[4] P. Piagi, R. H. Lasseter. Autonomous control of microgrids. In *Proceedings of the IEEE Power Electronics Specialists General Meeting*, IEEE, Montreal, Que, Canada, pp. 8–16. 2006.

[5] R. Caldon, F. Rossetto, R. Turri. Analysis of dynamic performance of dispersed generation connected through inverter to distribution networks. In *Proceedings of the17th International Conference on Electricity Distribution*, CIRED, Barcelona, Spain, pp. 1–5, 2003.

[6] S. Barsali, M. Ceraolo, P. Pelacchi, D. Poli. Control techniques of dispersed generators to improve the continuity of electricity. In *Proceedings of IEEE Power Engineering Society Winter Meeting*, IEEE, New York, USA, pp. 789–794, 2002.

[7] B. Kroposki, C. Pink, R. DeBlasio, H. Thomas, M. Simoes, P. K. Sen. Benefits of power electronic interfaces for distributed energy systems. In *Proceedings of IEEE Power Engineering Society General Meeting*, IEEE, Montreal, Que, Canada, pp. 901–907, 2006.

[8] K. De Brabandere, K. Vanthournout, J. Driesen, G. Deconinck, R. Belmans. Control of microgrids. In *Proceedings of IEEE Power Engineering Society General Meeting*, IEEE, Tampa, Florida, USA, pp. 1–7, 2007.

[9] K. De Brabandere, B. Bolsens, J. Van den Keybus, A. Woyte, J. Driesen, R. Belmans. A voltage and frequency droop control method for parallel inverters. *IEEE Transactions on Power Electronics*, vol. 22, no. 4, pp. 1107–1115, 2007.

[10] G. Weiss, Q. C. Zhong, T. C. Green, J. Liang. H_∞ repetitive control of DC-AC converters in microgrids. *IEEE Transactions on Power Electronics*, vol. 19, no. 1, pp. 219–230, 2004.

[11] E. Serban, H. Serban. A control strategy for a distributed power generation microgrid application with voltage- and current-controlled source converter. *IEEE Transactions on Power Electronics*, vol. 25, no. 12. pp. 2981–2992, 2010.

[12] D. Feng, Z. Chen. System control of power electronics interfaced distribution generation units. In *Proceedings of the 5th CES/IEEE International Power Electronics and Motion Control Conference* (IPEMC), IEEE, Shanghai, China, pp. 1–6, 2006.

[13] X. D. Hao, Q. S. Zeng. H_∞ output feedback control for stochastic systems with mode-dependent time-varying delays and Markovian jump parameters. *International Journal of Automation and Computing*, vol. 7, no. 4. pp. 447–454, 2010.

[14] Y. G. Chen, W. L. Li. Improved results on robust H_∞ control of uncertain discrete-time systems with time-varying delay. *International Journal of Automation and Computing*, vol. 6, no. 1, pp. 103–108, 2009.

[15] S. Xin, Q. L. Zhang, C. Y. Yang, Z. Su, Y Y. Shao. An improved approach to delay-dependent robust stabilization for uncertain singular time-delay systems. *International Journal of Automation and Computing*, vol. 7, no. 2, pp. 205–212, 2010.

[16] M. C. Chandorkar, D. M. Divan, R. Adapa. Control of parallel connected inverters in standalone AC supply systems. *IEEE Transactions on Industry Applications*, vol. 29, no. 1, pp. 136–143, 1993.

Chun-Xia Dou received the B. Sc. degree, the M. Sc. degree, and the Ph. D. degree from the Yanshan University, Qinhuangdao, China. She is currently a professor at the Institute of Electrical Engineering, Yanshan University.

Her research interests include control for smart grid, control for microgrid, and stability of wide-area power systems.

E-mail: cxdou@ysu.edu.cn (Corresponding author)

Fang Zhao received the B. S. degree from the Inner Mongolia University of Technology, Hohhot, China in 2009. She is currently a master student in the Institute of Electrical Engineering, Yanshan University, Qinhuangdao, China.

Her research interests include switched systems control and microsource control.

E-mail: nanwangzhaofang@163.com

Xing-Bei Jia received the B. Sc. degree from the Yanshan University, Qinhuangdao, China, in 2009. She is currently a master student in the Institute of Electrical Engineering, Yanshan University, Qinhuangdao, China.

Her research interests include optimization control, adaptive control, and transient stability control for power systems.

E-mail: jiaxingbei1986@163.com

Dong-Le Liu received the B. Sc. degree from the Yanshan University, Qinhuangdao, China in 2009. He is currently a master student in the Institute of Electrical Engineering, Yanshan University, Qinhuangdao, China.

His research interests include control for wind power systems and adaptive control.

E-mail: dongle668@163.com